



Engineering Applications of Computational Fluid Mechanics

ISSN: (Print) (Online) Journal homepage: <https://www.tandfonline.com/loi/tcfm20>

Comparison of the efficacy of particle swarm optimization and stochastic gradient descent algorithms on multi-layer perceptron model to estimate longitudinal dispersion coefficients in natural streams

Tao Hai, Hongwei Li, Shahab S. Band, Sadra Shadkani, Saeed Samadianfard, Sajjad Hashemi, Kwok-Wing Chau & Amir Mousavi

To cite this article: Tao Hai, Hongwei Li, Shahab S. Band, Sadra Shadkani, Saeed Samadianfard, Sajjad Hashemi, Kwok-Wing Chau & Amir Mousavi (2022) Comparison of the efficacy of particle swarm optimization and stochastic gradient descent algorithms on multi-layer perceptron model to estimate longitudinal dispersion coefficients in natural streams, Engineering Applications of Computational Fluid Mechanics, 16:1, 2207-2221, DOI: 10.1080/19942060.2022.2141896

To link to this article: <https://doi.org/10.1080/19942060.2022.2141896>



© 2022 The Author(s). Published by Informa UK Limited, trading as Taylor & Francis Group



Published online: 18 Nov 2022.



Submit your article to this journal [↗](#)



Article views: 844



View related articles [↗](#)



View Crossmark data [↗](#)

Comparison of the efficacy of particle swarm optimization and stochastic gradient descent algorithms on multi-layer perceptron model to estimate longitudinal dispersion coefficients in natural streams

Tao Hai^{a,b,c}, Hongwei Li^d, Shahab S. Band^e, Sadra Shadkani^f, Saeed Samadianfard^g, Sajjad Hashemi^f, Kwok-Wing Chau^g and Amir Mousavi^{h,i,j}

^aSchool of Computer and Information, Qiannan Normal University for Nationalities, Duyun, Guizhou, People's Republic of China; ^bCollege of Artificial Intelligence, Nanchang Institute of Science and Technology, Nanchang, People's Republic of China; ^cInstitute for Big Data Analytics and Artificial Intelligence (IBDAI), Universiti Teknologi MARA, 40450 Shah Alam, Selangor, Malaysia; ^dSchool of Information Engineering, Yulin university, Yulin, People's Republic of China; ^eFuture Technology Research Center, College of Future, National Yunlin University of Science and Technology, Yunlin, Taiwan; ^fDepartment of Water Engineering, Faculty of Agriculture, University of Tabriz, Tabriz, Iran; ^gDepartment of Civil and Environmental Engineering, Hong Kong Polytechnic University, Hong Kong, People's Republic of China; ^hObuda University, Budapest, Hungary; ⁱSlovak University of Technology in Bratislava, Bratislava, Slovakia; ^jInstitute of Information Society, University of Public Service, Budapest, Hungary

ABSTRACT

Accurate estimation of the longitudinal dispersion coefficient (LDC) is essential for modeling the pollution status in rivers. This research investigates the capabilities of machine-learning methods such as multi-layer perceptron (MLP), multi-layer perceptron trained with particle swarm optimization (MLP-PSO), multi-layer perceptron trained with Stochastic gradient descent deep learning (MLP-SGD) and different regressions including linear and non-linear regressions (LR and NLR) methods for determining the LDC of pollution in natural rivers and evaluates the accuracy of these methods in comparison with real measured data. Furthermore, the correlation coefficient (CC), root mean squared error (RMSE) and Willmott's Index (WI) were implemented to evaluate the accuracies of the mentioned methods. Comparison of the results showed the superiority of the MLP-SGD model with CC of 0.923, RMSE of 281.4 and WI of 0.954, which indicates the undeniable accuracy and quality of the deep-learning model that can be used as a powerful model for LDC simulation. Also due to the acceptable performance of the PSO algorithm in the hybridization of the MLP model, the use of PSO algorithms is recommended to train machine-learning techniques for LDC estimation.

ARTICLE HISTORY

Received 12 July 2021
Accepted 25 October 2022

KEYWORDS

Longitudinal dispersion coefficient; multi-layer perceptron; particle swarm optimization; stochastic gradient descent; deep learning; statistical evaluation




1. Introduction

Nowadays, one of the most important environmental subjects in the world is the study of surface water and river quality. Since rivers and surface waters are the main sources of water supply for different purposes, it is significant to determine and protect their quality. The main causes of surface water pollution are sewage and industrial wastes and the use of pesticides and insect killers in agriculture. On the other hand, other problems such as drought damage make it necessary to study the issue of water quality.

As mentioned, the entry of various agricultural and industrial wastes into rivers and streams has become a common way to dissolve and eliminate biological matter. One of the solutions that can be applied to control pollution in open channel streams is the effluence

of contaminants in a controlled and logical mode that enables the utilization of the process of dispersion and self-purification of the river, which is one of the most important methods of river environmental management, to decrease the damage to the environment. Therefore, it is necessary to have sufficient and accurate knowledge of the ability of water to carry, spread and clean the contamination along a certain length of its path, which is called the full mixing length.

Pollutants are released under the effect of transfer and mixing processes in vertical, transverse and longitudinal directions. Capability and strength of rivers and other surface flows in the distribution of additional materials in longitudinal, transverse and vertical directions are expressed by dispersion coefficients K_x , K_y and K_z , respectively (Tayfur & Singh, 2005). K_x is the

CONTACT Saeed Samadianfard  s.samadian@tabrizu.ac.ir; Shahab S. Band  shamshirbands@yuntech.edu.tw;
Amir Mosavi  amir.mosavi@kvk.uni-obuda.hu

most important coefficient, which has a significant effect on farther distances as well (Chatila, 1997). Therefore, appropriate and accurate evaluation of longitudinal dispersion coefficient (LDC) is one of the main prerequisites for the study of variations in the concentration of contaminants in natural rivers. Also, accurate modeling and estimation of this coefficient has special position in reservoirs and deltas designing, environmental issues and river engineering (Fischer et al., 1979). The LDC can be easily specified in the presence of real data, but unknown features and characteristics of mixing and dispersion in most rivers have forced researchers to use different experimental relations. Some experimental and theoretic approaches that have been extensively developed, comprise those by Elder (1959), Fisher (1968, 1975), McQuivey and Keefer (1974), Liu (1977), Fischer et al. (1979), Iwasa and Aya (1991), Seo and Cheong (1998), Kashefipour and Falconer (2002) and Disley et al. (2015). Although empirical equations are valuable, they have disadvantages such as low accuracy and high cost. Also, each of these relations considers only some of the effective parameters and a comprehensive relation has not yet been accepted by all researchers which comprises all the effective parameters. In recent years, in addition to the use of these equations, the implementation of artificial intelligence methods that are highly accurate has attracted the attention of many river engineers and researchers.

Kargar et al. (2020) investigated multiple linear regression, random forest, M5 model tree (M5P), Gaussian process regression and support vector regression to modeling LDC in 60 natural streams of different regions around the world. They used various geometric and hydraulic information of the study area as model input and compare the result with empirical models. It was concluded that the established M5P technique had better accuracy in comparison with empirical equations and other machine-learning techniques. Noori et al. (2009) estimated the LDC applying adaptive neuro-fuzzy inference system (ANFIS) and support vector machine (SVM) models. Results indicated that the established models were superior to classical regression methods. In another study, LDC was forecasted by genetic programming method in natural rivers. The developed genetic programming method created precise results ($RMSE = 0.085$ and $R^2 = 0.98$) (Azamathulla & Ghani, 2011). Tayfur and Singh (2005) calculated the LDC in natural rivers and streams implementing artificial neural network (ANN) technique. The model input variables include geometric features (channel shape parameter, channel sinuosity, and channel width) and hydraulic parameters (relative shear velocity, shear velocity, flow velocity, flow depth, and flow discharge). They indicated

that the developed ANN model can be more useful than empirical formulas in prediction of LDC. Sattar and Gharabaghi (2015) presented a new gene expression model to establish experimental relations between the LDC and different control parameters in rivers of New Zealand, Europe, Canada, and the United States. Findings displayed that the developed models are accurate and can be efficiently utilized to forecast the LDC in the studied areas. In the research of Antonopoulos et al. (2015), an empirical equation and ANN model were developed for dispersion coefficient estimation based on various hydrodynamic and hydrological information of Axios River. They presented that the ANN models showed results with acceptable accuracy. Applying MLP and the radial basis function (RBF) techniques and empirical equations, Parsaie and Haghiabi (2015) forecasted the LDC in rivers and revealed that MLP and RBF models had appropriate performance for estimating LDC. Najafzadeh and Tafarjoruz (2016) examined the capabilities of neuro-fuzzy-based group method of data handling (NF-GMDH) and enhanced this method by means of particle swarm optimization algorithms (PSO) in LDC estimation. The comparison of the NF-GMDH-PSO results with the results of artificial neural network (ANN), model tree (MT), and the differential evolutionary (DE) displayed that DE model as superior technique. Alizadeh et al. (2017) considered Bayesian network (BN) method for estimation of LDC based on two types of input data covering dimensionless and dimensional variables. The established technique provided an appropriate method for pollutant transport prediction in natural streams. Mohammad Najafzadeh et al. (2021) performed uncertainty analysis in estimation of longitudinal and lateral dispersion coefficients (K_x and K_y) in rivers. For this purpose, they implemented five intelligent models for estimation of the mentioned coefficients. They reported that support vector machine gives least uncertainty in both K_x and K_y estimation. Ghiasi et al. (2021) suggested implementing Deep Convolutional Network (DCN) for improving the accuracy of LDC estimation. They stated that the utilized DCN model demonstrates exceptional accuracy in estimating LDC over the full possible range of data in comparison with the empirical and ML models. Naser Arya Azar et al. (2021) used least square-support vector machine (LS-SVM), adaptive neuro-fuzzy inference system (ANFIS), and ANFIS optimized by Harris hawk optimization (ANFIS-HHO) for LDC estimation and they compared the results with that of the experimental methods. The obtained results exhibited that the proposed ANFIS-HHO performed better than the other two models. The superiority of artificial intelligence and machine-learning methods over experimental equations in estimating longitudinal scattering coefficient has also

been expressed in other studies (Azamathulla & Wu, 2011; Najafzadeh & Sattar, 2015; Noori et al., 2011, 2015; Piotrowski et al., 2012; Riahi-Madvar et al., 2009; Sahay, 2011; Toprak et al., 2004, 2014; Toprak & Cigizoglu, 2008)

The special position of LDC in contamination transfer and its dependency on geometric and hydrodynamic factors can be concluded from the number of studies that have been conducted over the past decades until now (Altunkaynak, 2016; Bencala & Walters, 1983; Deng et al., 2001; Etemad-Shahidi & Taghipour, 2012; Rutherford, 1994; Tutmez & Yuceer, 2013; Wang et al., 2017).

The main purpose of this study is to investigate different experimental methods and equations for accurate estimation of LDC in natural rivers and to evaluate the performance accuracy of these methods in comparison with real measured data. So, the main contribution of this study is evaluating MLP-SGD deep learning and PSO algorithm to improve the accuracy of standalone MLP in LDC estimation. Finally, the results of empirical equations and LR and NLR models are compared with each other.

2. Material and methods

2.1. Database used

Estimation of longitudinal dispersion coefficient using experimental equations requires a set of hydraulic and geometric data of the rivers. In this study, data from 50 different rivers in the US and the UK (see Appendix), which have been used in different sources have been gathered (Fisher, 1968; Graf, 1995; McQuivey & Keefer, 1974; Nordin & Sabol, 1974; Rutherford, 1994). The dataset includes flow depth (m), river width (m), average flow velocity (m/s), flow shear velocity (m/s), and ε (m²/s). Table 1 presents the variables required for the experimental equations, the parameters used for modeling, and the statistical parameters of the data used.

2.2. Models used in the research

The use of dimensional analysis method and presentation of dimensionless variables allows more detailed study of the factors affecting the relationships governing the LDC. The most important parameters that affect the diffusion phenomenon are three categories of fluid properties (density fluid (ρ), fluid viscosity coefficient (μ)), hydraulic characteristics of flow (average flow velocity (U), flow depth (h) and flow shear rate (U_*)) and geometric parameters of flow cross section (river width (w), flow path shape, etc.). in other words:

$$\varepsilon = f_1(u, h, w, U_*, \rho, \mu) \quad (1)$$

Equation 2 can be obtained by using Buckingham theorem.

$$\frac{\varepsilon}{HU_*} = f_2\left(\frac{U}{U_*}, \frac{W}{H}, Re^*\right) \quad (2)$$

ε/HU_* is dimensional mixing or dispersion coefficient without dimension and Re^* is the shear Reynolds number. If the turbulent flow is rough ($Re^* \geq 70$), the effect of fluid viscosity can be disregarded and Equation 2 can be summarized as Equation 3.

$$\frac{\varepsilon}{HU_*} = f_2\left(\frac{U}{U_*}, \frac{W}{H}\right) \quad (3)$$

For this reason, the existing experimental equations use the parameters of dimensionless velocity and dimensionless flow depth to estimate this coefficient.

2.3. Experimental equations

In order to estimate the LDC in the rivers, researchers presented various experimental relationships, the most important of which are presented in Table 2. As can be seen, all of these formulas calculate the LDC using variables related to the average flow conditions in the river section.

2.4. Feed-Forward multi-layer perceptron (MLP)

In this study, forward multilayer perceptron neural networks were used to estimate LDC. This network is made up of simple operational elements called neurons that work in parallel. Multilayer neural networks consist of an input layer (for input data), one or more hidden layers (for organizing neurons), and an output layer (for output data). The function of the neural network is determined by how the components are connected, by adjusting the values of each connection, which is called the connection weight. One of the most widely used types of neural networks in hydrology and water resources is feed-forward multilayer perceptron neural networks with back propagation error training pattern (Ulke et al., 2009). In this type of neural networks, the direction of data flows from the input layers towards the hidden layers as described as follows by (Tayfur, 2012).

$$w_{ij}^{new} = w_{ij}^{old} - \eta \frac{\partial E}{\partial w_{ij}} \quad (4)$$

Where w_{ij}^{old} and w_{ij}^{new} are the weights between neurons i and j , respectively, before and after a given repetition, η is the learning rate, and E is the error function. Network training and error reduction continue until network convergence is established. Neural networks can have

Table 1. Statistical characteristics of utilized data.

Parameters	Mean	Minimum	Maximum	Standard deviation	Coefficient of variation	Skewness
W(m)	49.582	1.4000	253.600	48.285	0.973	2.160
H(m)	1.476	0.14	20.900	2.071	1.403	6.195
U(m/s)	0.473	0.029	1.730	0.318	0.672	1.595
U_* (m/s)	0.084	0.0016	0.553	0.072	0.851	3.925
ε (m ² /s)	83.294	0.200	1486.500	180.954	2.172	4.791
W/H	47.308	2.202	403.750	46.852	0.990	4.437
U/U _*	7.000	0.777	20.250	4.652	0.664	1.277
ε/HU_*	1210.855	3.083	37140.740	3629.165	2.997	7.944

Table 2. Empirical equations for LDC estimation.

Method	Equation	Notation
Seo and Cheong (1998)	$\frac{\varepsilon}{HU_*} = 5.915 \times \left(\frac{W}{H}\right)^{0.62} \times \left(\frac{U}{U_*}\right)^{1.428}$	S-C
Li, Liu, and Yin (2013)	$\frac{\varepsilon}{HU_*} = 2.282 \times \left(\frac{W}{H}\right)^{0.7613} \times \left(\frac{U}{U_*}\right)^{1.4713}$	L
Zeng and Huai (2014)	$\frac{\varepsilon}{HU_*} = 5.4 \times \left(\frac{W}{H}\right)^{0.7} \times \left(\frac{U}{U_*}\right)^{1.13}$	Z-H
Zhang, Huai, and Zhao (2016)	$\frac{\varepsilon}{HU_*} = 17.648 \times \left(\frac{W}{H}\right)^{0.3619} \times \left(\frac{U}{U_*}\right)^{1.16}$	W-H
Kargar et al. (2020)	$\frac{\varepsilon}{HU_*} = 1.6896 \times \left(\frac{W}{H}\right) + 20.0124 \times \left(\frac{U}{U_*}\right) + 393.3346$ If $\frac{W}{H} \leq 47.238$ $\frac{\varepsilon}{HU_*} = 2.8759 \times \left(\frac{W}{H}\right) + 181.7915 \times \left(\frac{U}{U_*}\right) + 339.5557$ If $\frac{W}{H} > 47.238$	K

multiple hidden layers, however, research shows that forward neural networks, with a hidden layer, are able to approximate any nonlinear function (Hornik et al., 1989).

2.5. Particle swarm optimization (PSO)

The Particle Swarm Optimization (PSO) algorithm is a social search algorithm inspired by the social behavior of birds and fishes when searching for food. In this algorithm, each solution (in this study, the weights and biases of the neural network), which is also called a particle, is equivalent to a bird in a pattern in the collective movement of birds and it is determined by a target function. In the PSO algorithm, the particles work together to achieve a common goal, so this method is more effective when the particles act separately. In the PSO algorithm, collective behavior is not only related to the behavior of the individual in the community but also to how the group interacts. So, the particles are spread in the search space, then in order to achieve the best solutions, under the influence of their own experience and knowledge and the knowledge of other particles of their neighbors, gradually tend to successful areas (optimal solutions). Compared to other evolutionary algorithms, the PSO algorithm has interesting features such as constructive collaboration and shared memory between individuals. Therefore, in this algorithm, moving to areas containing better solutions has a better chance and discovering solutions with the desired quality is faster. In

addition, this algorithm is very simple and has high speed and low memory. Moreover, first a number of particles are created with random position and speed, then in each iteration; the particles correct the movement toward the target according to the best position of their past and their neighbors. After consecutive repetitions, the problem converges to the optimal answer. The correction of the velocity and position of each particle is done by the Equations 5 and 6, respectively as described by Marini and Walczak (2015).

$$\begin{aligned}
 V_{i+1}(t+1) &= \omega V_i(t) + C_1 \\
 &\quad \times (rand_1(pbest_i(t) - X_i(t))) \\
 &\quad + C_2 \times (rand_2(gbest_i(t) - X_i(t))) \quad (5) \\
 X_i(t+1) &= X_i(t) + V_i(t+1) \quad (6)
 \end{aligned}$$

In which *gbest* represents the best position obtained by the particle population and *pbest* represents the best position the particle itself has ever experienced, *t* represents the number of iterations, *c* represents the acceleration constant and *rand1* and *rand2* are random numbers in the range zero and 1. The coefficients *C*₁ and *C*₂ are cognitive parameter (personal experience) and social parameter (collective experience), respectively, and determine the slope of movement in local search. The value of these two coefficients is determined in the range of zero and 2. Moreover, ω is a coefficient that decreases linearly and is usually defined in the range of zero and 1. The operation

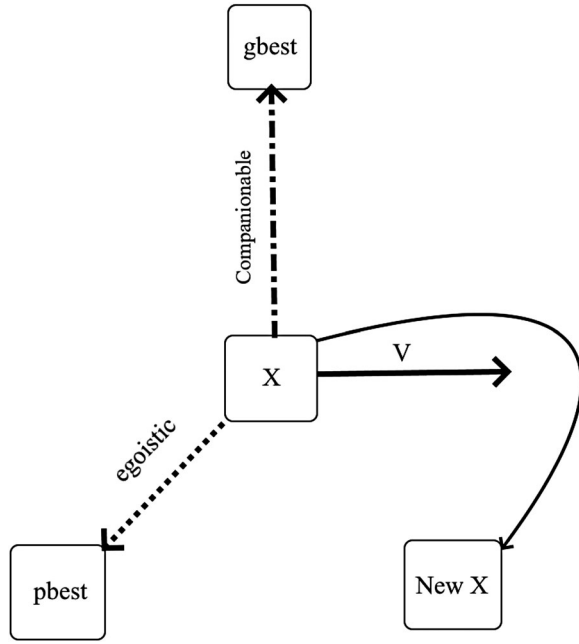


Figure 1. Performance of PSO algorithm.

of the PSO algorithm, which is adapted from Marini and Walczak (2015) is shown in Figure 1.

2.6. Application of PSO algorithm in optimization and training of neural networks

In the neural network training, optimization variables include the weights and biases of that network. If the n th layer of a hypothetical neural network consisting of input R and M neurons is considered, then the matrix of weights (W^n) and biases (B^n) of this layer can be represented using as follows:

$$W^n = \begin{bmatrix} (W_1^n)^T \\ (W_2^n)^T \\ \vdots \\ (W_M^n)^T \end{bmatrix}, B^n = \begin{bmatrix} b_1^n \\ b_2^n \\ \vdots \\ b_M^n \end{bmatrix} \quad (7)$$

Where $[W_{m,1}^n \ W_{m,2}^n \ \dots \ W_{m,R}^n]^T$ is the vector of the weights that the m neuron relates to the inputs of the same layer. The vector of the parameters of this layer can also be shown with Equation 8.

$$X^n = \begin{bmatrix} W_1^n \\ \vdots \\ W_M^n \\ - \\ b_1^n \\ \vdots \\ b_M^n \end{bmatrix} \quad (8)$$

Similarly, for each layer in the neural network, the weight and bias matrices and vectors of the corresponding parameters are defined. By subtracting the vector parameters of all network layers, the vector of the desired optimization variables is formed. Finally, for a network with L layer, the vector of X variables can be obtained from the equation 9.

$$X = \begin{bmatrix} X^1 \\ X^2 \\ \vdots \\ X^L \end{bmatrix} \quad (9)$$

where the vector represents the particle position as the optimal value. The position vector N of X_i ($i = 1, 2, \dots, N$), represents the quantity of the members of the particle solutions. The neural network further operates for parameters of the vectors' variables. As described by Garro and Vázquez (2015) the equations 5 and 6 in the next step are used for calculation of the new position vectors.

2.7. Multilayer perceptron-stochastic gradient descent (MLP-SGD)

Stochastic gradient descent (SGD) is a repeating method for improving a purpose function with proper softness properties. To estimate the gradient in the gradient descent (GD), the average of all n samples must be obtained. If the training dataset consists of millions or billions of samples, the average will be difficult to calculate, so each iteration will be long. SGD is used to prevent such a problem. In other words, in each iteration, a sample of a micro-batch M is sampled from n samples in the training dataset. These samples are uniformly sampled from the training dataset and the size of n is constant and relatively smaller than n . To update all parameters, a gradient is estimated for all pairs of specimens in the M sub-category. The SGD training transforms to gradient descent when the batch size is n . In the SGD method the parameters are upgraded more repeatedly than for the gradient descent, and the convergence is rummaged. When the batch size is 1, the maximum iteration of upgrades is done, leading to an ordinary perceptron-like algorithm (Tsuruoka et al., 2009). In this case, the equivalent of the gradient estimate for any data such as $x^{(i)}$ and its corresponding value $y^{(i)}$ would be as follows:

$$g_{\text{SGD}} = \frac{1}{n} \sum_{i=1}^n \nabla_{\theta} \zeta(x^{(i)}, y^{(i)}, \theta_t) \quad (10)$$

After estimating the gradient, the parameter is updated in the opposite direction of the gradient:

$$\theta_{t+1} = \theta_t - \eta g_{\text{SGD}} \quad (11)$$

In Equation (11) η is the learning rate which decreases as the repetition process.

MLP-SGD is a MLP based method that is improved by SGD. The MLP-SGD network consists many hidden layers include neurons with a scaled sigmoid, rectifier, max out, and ExpRectifier activation functions. Progressed features such as epochs, rho, L1 or L2 adjustment, momentum training, adaptive learning rate, and rate annealing allow for high prediction precision. The mentioned parameters activate if the adaptive learning rate is disabled.

2.8. Error evaluation indicators

In order to evaluate and compare the results obtained from machine learning and regression models with observed LDC data, correlation coefficient (CC), root mean squared error (RMSE) and Willmott's Index (WI) were used. The equations of the indicators used are as follows:

$$CC = \frac{\left(\sum_{i=1}^n O_i P_i - \frac{1}{n} \sum_{i=1}^n O_i \sum_{i=1}^n P_i \right)}{\sqrt{\left(\sum_{i=1}^n O_i^2 - \frac{1}{n} \left(\sum_{i=1}^n O_i \right)^2 \right) \left(\sum_{i=1}^n P_i^2 - \frac{1}{n} \left(\sum_{i=1}^n P_i \right)^2 \right)}} \quad (12)$$

$$RMSE = \sqrt{\frac{1}{n} \sum_{i=1}^n (P_i - O_i)^2} \quad (13)$$

$$WI = 1 - \left[\frac{\sum_{i=1}^n (O_i - P_i)^2}{\sum_{i=1}^n (|P_i - \bar{O}_i| + |O_i - \bar{O}_i|)^2} \right] \quad (14)$$

where O_i and P_i are the measured and estimated values, respectively. \bar{O}_i represents the mean value of the observed values and n represents the number of data. The CC and WI values close to 1 and RMSE values close to 0 indicate the high quality of the LDC estimation. The Taylor diagrams with different colors at the polar poles (Taylor, 2001) are used to evaluate the model accuracy and the estimated values of LDC prediction.

3. Results and discussion

In the present study, 149 datasets belonging to 50 different rivers were used to model and estimate the LDC. Furthermore, there is no direct way for separating training and testing datasets. For example, for developing the model, Deo et al. (2018) and Samadianfard et al. (2019a, 2019b, 2020) implemented 70% of their data,

Table 3. Performance of S-C, L, Z-H, W-H and K empirical models based on utilized statistical parameters.

Models	Empirical models		
	CC	RMSE	WI
S-C	0.739	791.0	0.796
L	0.776	532.9	0.872
Z-H	0.774	454.8	0.863
W-H	0.640	550.3	0.772
K	0.774	674.8	0.800

while Qasem et al. (2019) applied 67%, Diop et al. utilized 75% and Zounemat-Kermani et al. (2019) used 80% of whole data for training step. Accordingly, 70% of data (104 cases) is used as training, and the rest of them (45 cases) are applied for the testing part. It is worth mentioning that the data were divided randomly.

Four-layer perceptron neural network (one input layer, two hidden layers and one output layer) was used to estimate LDC using MLP method. The Levenberg-Marquardt algorithm was implemented in estimating the LDC due to its efficiency and faster convergence in neural network training. Activation functions in latent and output layer neurons were considered sigmoid and linear, respectively. In order to use the PSO algorithm in this research, population size, maximum number of iteration, inertia weight and initial particles were considered 1000, 500, 0.9, and 30, respectively.

Using 30% of the dataset collected in this study, which was used to test the models, the LDC values were calculated using each of the relationships in Table 2 and their accuracy was evaluated using the measured data. Table 3 shows the results of the implemented empirical equations. Z-H is the most accurate empirical equation, with CC, RMSE and WI values of 0.774, 454.8, and 0.863, respectively, which shows the efficiency of this equation. Additionally, the proposed S-C equations have the lowest accuracy so that CC, RMSE, and WI values are 0.739, 791.0, and 0.796, respectively. The high value of RMSE indicates the inefficiency of this equation. Efficiency or inefficiency of these equations can be deduced from the scatter and comparison plots that have presented in Figures 2 and 3.

Additionally, Table 4 represents the evaluation meters of MLP, MLP-PSO, MLP-SGD, and regression methods. Accordingly, the best performance belongs to the MLP-SGD with CC of 0.923, RMSE of 281.4, and WI of 0.954. Thus, MLP-SGD had high potential compared to other models for low-error modeling of LDC values. On the other hand, according to the results obtained from MLP-PSO model, the use of PSO algorithm in MLP neural network training improved the performance of the MLP neural network model, so that all values of the validation indices of the standalone MLP model have

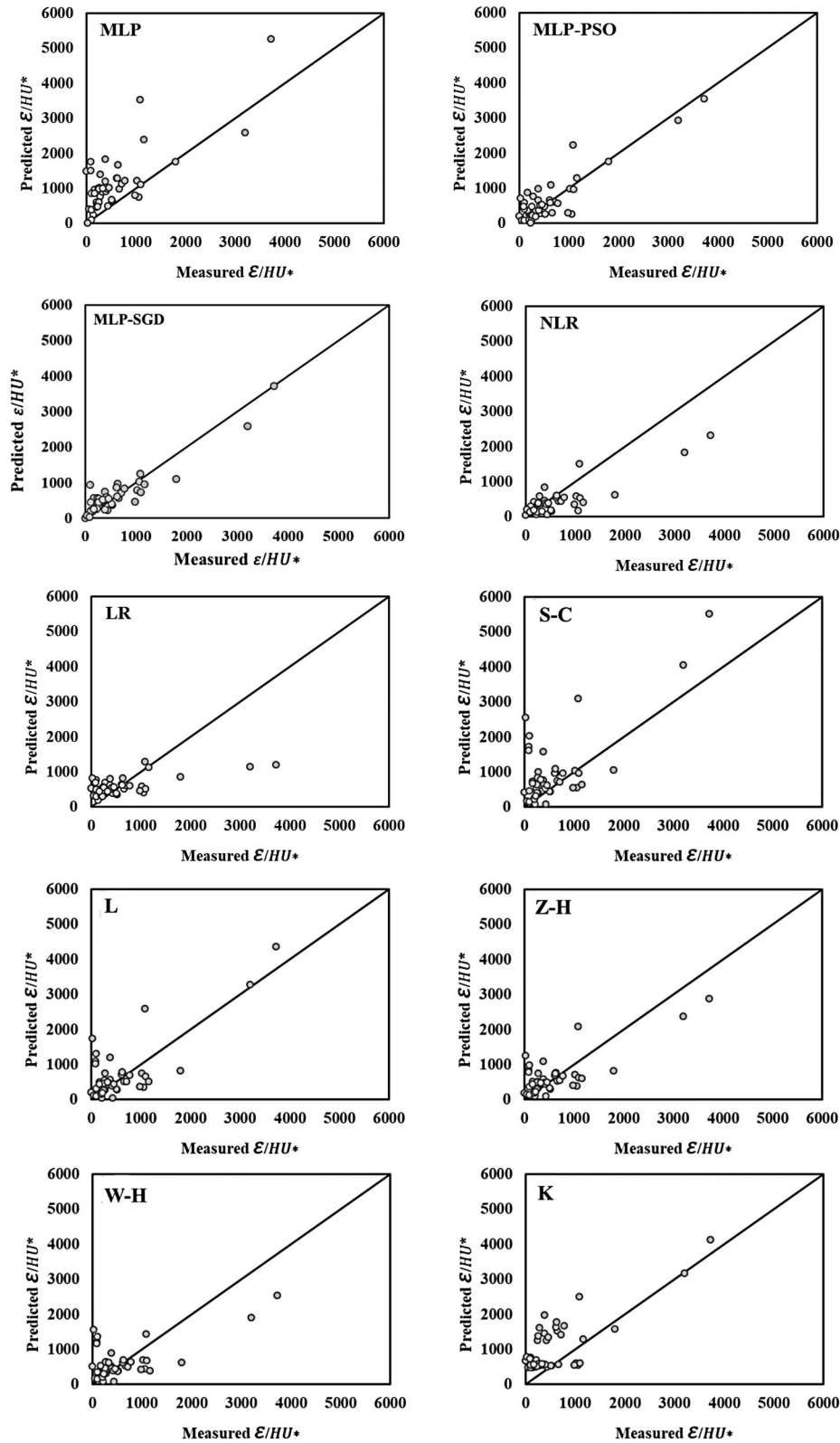


Figure 2. Scatterplots of measured and estimated LDC.

improved. To better understand, the CC, RMSE, and WI values have changed from 0.769–0.884, 803.6–347.8, and 0.775–0.937, respectively. In other words, these parameters have improved by 14.9%, 56.7%, and 20.9% respectively.

Regression equations for LDC estimation were obtained using LR and NLR methods and presented in Table 5. These equations depend on the values of W/H and U/U_* . According to the results shown in Table 4,

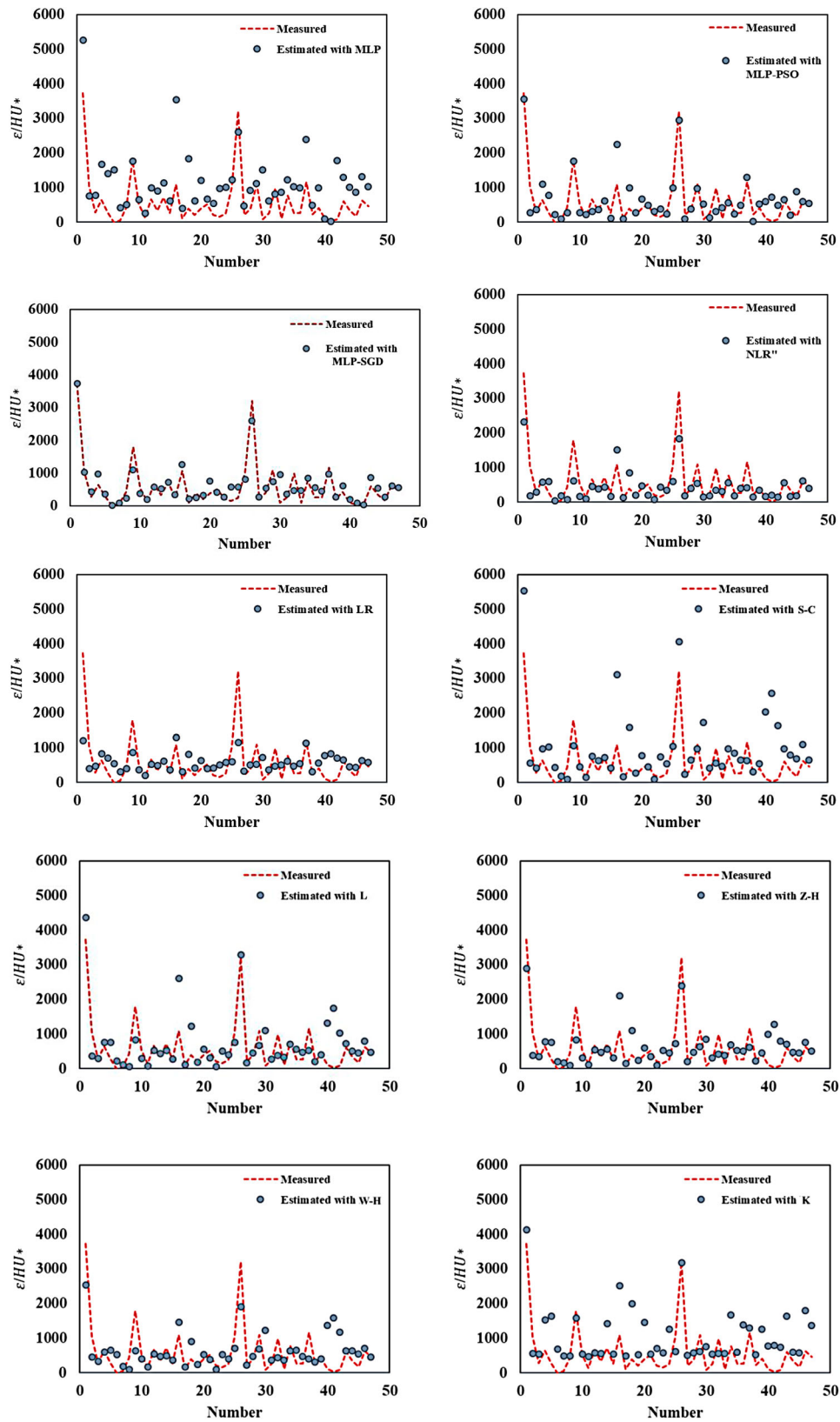


Figure 3. Comparative plots of measured and estimated LDC.

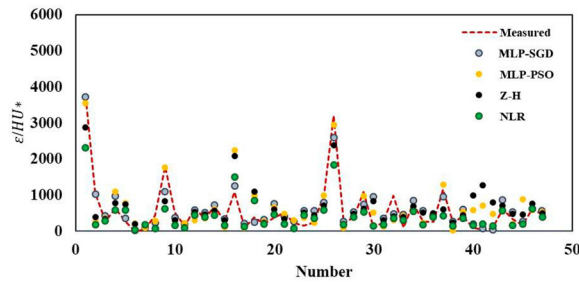


Figure 4. Comparative graph between superior methods.

the performance accuracy of the NLR with CC of 0.864, RMSE of 431.7, and WI of 0.856 and LR with CC of 0.639, RMSE of 590.0, and WI of 0.584 are lower than the optimized MLP-PSO method. But due to the reasonable error of the NLR method, the resulted equation of NLR may be proposed for LDC estimation. It should be noted that the equation presented by NLR method was presented in two domains of $W/H > 29$ and $W/H \leq 29$. By comparing the results of Table 4 with Table 3, it can be concluded that the performance of NLR is superior to the empirical equations examined in this study. Scatter and comparative plots of the implemented methods are shown in Figures 2 and 3. As can be seen from Figures 2 and 3, the scatter of points (light blue points) around the bisector line (solid black line) of the MLP-SGD are lower than other methods. Furthermore, the conformity of the estimated points (dark blue points) on the measured data line (red dotted line) in the MLP-SGD model is more than others, which indicates the superiority of the MLP-SGD model.

To compare the superior methods between empirical and machine-learning models and to identify the most efficient method, Figure 4 was drawn to compare the results of Z-H and the MLP-PSO, MLP-SGD, and NLR machine-learning methods that the proximity of the points related to the MLP-SGD (pale blue points) to the observed data line (red dotted line) showed the suitability of this method for estimating LDC. Moreover, Figure 5

Table 4. Performance of MLP, MLP-PSO, MLP-SGD, LR and NLR models based on utilized statistical parameters.

Models	Machine learning models		
	CC	RMSE	WI
MLP	0.769	803.6	0.775
MLP-PSO	0.884	347.8	0.937
MLP-SGD	0.923	281.4	0.954
LR	0.639	590.0	0.584
NLR	0.864	431.7	0.856

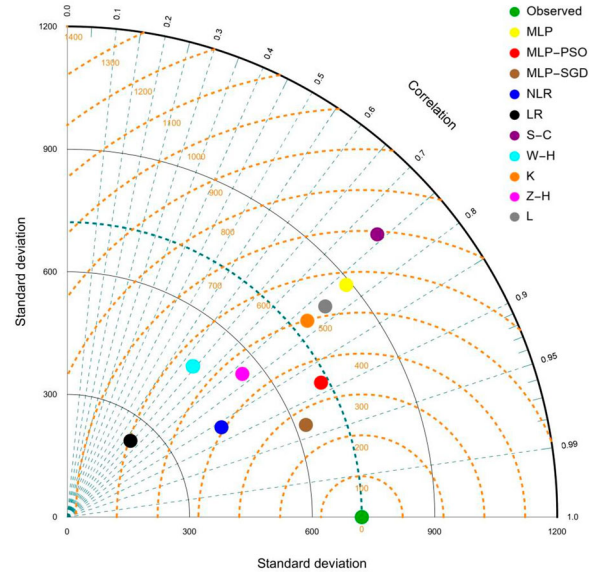


Figure 6. The Taylor diagrams of observed and estimated LDC values.

demonstrates the boxplots of the utilized models. Similarly, it is clear that the estimates of MLP-SGD are in better agreement with the measured LDC values.

In Figure 6, the Taylor diagrams of models are illustrated where the RMSE is presented as the distance from the reference point. The model with high accuracy is considered as less distance between reference and the correspondent point. As the brown point for MLP-SGD is

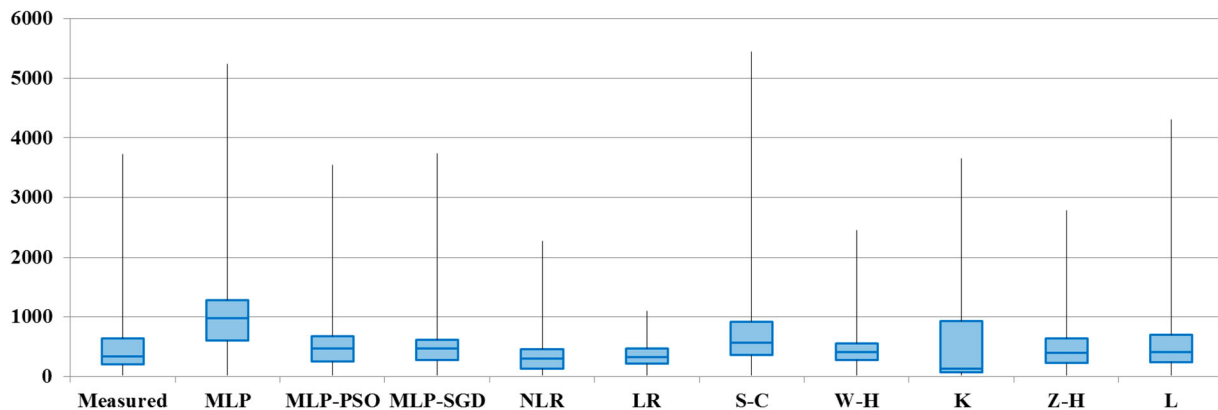


Figure 5. Boxplots of measured and estimated LDC.

Table 5. Linear and nonlinear regression equations obtained to estimate the LDC.

Method	Equation	Data domain
Linear regression	$\frac{\varepsilon}{HU_*} = 7.751 \times \left(\frac{W}{H}\right) + 35.906 \times \left(\frac{U}{U_*}\right) + 0.011$	
Non- linear regression	$\frac{\varepsilon}{HU_*} = 7.112 \times \left(\frac{W}{H}\right)^{0.561} \times \left(\frac{U}{U_*}\right)^{1.158}$	$\frac{W}{H} > 29$
	$\frac{\varepsilon}{HU_*} = 19.011 \times \left(\frac{W}{H}\right)^{0.635} \times \left(\frac{U}{U_*}\right)^{0.139}$	$\frac{W}{H} \leq 29$

Table 6. Effect of removing input variables on the accuracy of MLP-SGD model in LDC estimation.

Model	(MLP-SGD) Input Parameters	Statistical Parameter		
		CC	RMSE	WI
1	All	0.923	281.4	0.954
2	Remove $\frac{W}{H}$	0.361	677.2	0.372
3	Remove $\frac{U}{U_*}$	0.503	583.1	0.526

the nearest point to the reference point, it delivers more accuracy.

Comparing the results of this study with the findings of Kargar et al. (2020) indicated that the developed MLP-SGD model (with RMSE of 281.4) estimated LDC with higher accuracy than M5P (with RMSE of 454.9), as the best model of Kargar et al. (2020). So, based on the outcomes of this research, the proposed MLP-SGD may be recommended for LDC estimation with high degree of confidentiality.

4. Sensitivity analysis

Sensitivity analysis indicates the effect of different input parameters of the model, in which the values of each parameter include the range of that parameter, which is located between the lower and upper limits of the range of changes of that parameter; In this way, one parameter changes between its lower and upper limit, while the other parameter remains constant in its average. The results of sensitivity analysis showed that the importance of the flow-to-depth ratio (W/H) is higher than U/U_* for estimating LDC using the most accurate model (MLP-SGD). This importance is due to the removal of this parameter from LDC modeling, which resulted in 60.9% decrease in CC, 140.6% increase in RMSE, and 61.0% decrease in WI indices, while these changes are 42.0% decrease in CC, 107.2% increase in RMSE and 44.9% decrease in WI indices by removing U/U_* . The complete results of the sensitivity analysis can be seen in Table 6.

5. Conclusion

Proper estimation of longitudinal dispersion coefficient of pollution is very important due to its undeniable

effect on pollution control and management in rivers. In this study, the LDC values were estimated through several experimental equations and machine learning and regression methods such as MLP, MLP-PSO, MLP-SGD, NLR, and LR and their accuracy were evaluated using the measured data. To achieve this goal, 149 datasets belonging to 50 rivers in the United States and the United Kingdom were divided into two parts: 70% training and 30% testing. Among the experimental methods, the Z-H had the best performance with the CC of 0.774, the RMSE of 454.8, and WI of 0.863. Among machine-learning methods, the MLP-SGD method showed highest accuracy with CC of 0.923, RMSE of 281.4, and WI of 0.954. Also the MLP-PSO method indicated acceptable accuracy with CC of 0.884, RMSE of 347.8, and WI of 0.937. Therefore, it may be concluded that the PSO algorithm had a significant effect on improving the results of the standalone MLP method, which indicates the efficiency of this optimization algorithm. Using NLR and LR methods, equations for LDC estimation were presented, which NLR equations in two domains with CC of 0.864, RMSE of 431.7, and WI of 0.856 had acceptable accuracy. Thus, LDC can be estimated by these non-linear equations considering low error values. Finally, due to the importance of estimating LDC as accurately as possible, the use of deep-learning methods and PSO optimization algorithms is recommended.

Disclosure statement

No potential conflict of interest was reported by the author(s).

ORCID

Saeed Samadianfard  <http://orcid.org/0000-0002-6876-7182>

Kwok-Wing Chau  <http://orcid.org/0000-0001-6457-161X>

Amir Mousavi  <http://orcid.org/0000-0003-4842-0613>

References

- Alizadeh, J. M., Shahheydari, H., Kavianpour, M. R., Shamloo, H., & Barati, R. (2017). Prediction of longitudinal dispersion coefficient in natural rivers using a cluster-based Bayesian network. *Environmental Earth Sciences*, 76(86), 1–11. <https://doi.org/10.1007/s12665-016-6379-6>

- Altunkaynak, A. (2016). Prediction of longitudinal dispersion coefficient in natural streams by prediction map. *Journal of Hydro-Environment Research*, 12, 105–116. <https://doi.org/10.1016/j.jher.2016.05.001>
- Antonopoulos, V. Z., Georgiou, P. E., & Antonopoulos, Z. V. (2015). Dispersion coefficient prediction using empirical models and ANNs. *Environmental Processes*, 2(2), 379–394. <https://doi.org/10.1007/s40710-015-0074-6>
- Arya Azar, N., Ghordoyee Milan, S., & Kayhomayoon, Z. (2021). The prediction of longitudinal dispersion coefficient in natural streams using LS-SVM and ANFIS optimized by Harris hawk optimization algorithm. *Journal of Contaminant Hydrology*, 240, 103781. <https://doi.org/10.1016/j.jconhyd.2021.103781>
- Azamathulla, H. M., & Ghani, A. A. (2011). Genetic programming for predicting longitudinal dispersion coefficients in streams. *Water Resources Management*, 25(6), 1537–1544. <https://doi.org/10.1007/s11269-010-9759-9>
- Azamathulla, H. M., & Wu, F.-C. (2011). Support vector machine approach for longitudinal dispersion coefficients in natural streams. *Applied Soft Computing*, 11(2), 2902–2905. <https://doi.org/10.1016/j.asoc.2010.11.026>
- Bencala, K. E., & Walters, R. A. (1983). Simulation of solute transport in a mountain pool-and-riffle stream: A transient storage model. *Water Resources Research*, 19(3), 718–724. <https://doi.org/10.1029/WR019i003p00718>
- Chatila, G. J. (1997). *Modeling of pollutant transfer in compound open channels*. Doctoral dissertation. University of Ottawa, Ontario, Canada.
- Deng, Z. Q., Singh, V. P., & Bengtsson, L. (2001). Longitudinal dispersion coefficient in straight rivers. *Journal of Hydraulic Engineering*, 127(11), 919–927. [https://doi.org/10.1061/\(ASCE\)0733-9429\(2001\)127:11\(919\)](https://doi.org/10.1061/(ASCE)0733-9429(2001)127:11(919))
- Deo, R. C., Ghorbani, M. A., Samadianfard, S., Maraseni, T., Bilgili, M., & Biazar, M. (2018). Multi-layer perceptron hybrid model integrated with the firefly optimizer algorithm for windspeed prediction of target site using a limited set of neighboring reference station data. *Renewable Energy*, 116, 309–323. <https://doi.org/10.1016/j.renene.2017.09.078>
- Disley, T., Gharabaghi, B., Mahboubi, A., & McBean, A. (2015). Predictive equation for longitudinal dispersion coefficient. *Hydrological Processes*, 29(2), 161–172. <https://doi.org/10.1002/hyp.10139>
- Elder, J. W. (1959). The dispersion of marked fluid in turbulent shear flow. *Journal of Fluid Mechanics*, 5(4), 544–560. <https://doi.org/10.1017/S0022112059000374>
- Etemad-Shahidi, A., & Taghipour, M. (2012). Predicting longitudinal dispersion coefficient in natural streams using M5' model tree. *Journal of Hydraulic Engineering*, 138(6), 542–554. [https://doi.org/10.1061/\(ASCE\)HY.1943-7900.0000550](https://doi.org/10.1061/(ASCE)HY.1943-7900.0000550)
- Fischer, B. H. (1975). Discussion of simple method for predicting dispersion in streams, by R.S McQuivey and T.N Keefer. *Journal of the Environmental Engineering Division*, 101(3), 453–455. <https://doi.org/10.1061/JEEGAV.0000360>
- Fischer, B. H., List, E. J., Koh, C. Y., Imberger, J., & Brooks, N. H. (1979). *Mixing in inland and coastal waters*. Academic Press Inc.
- Fisher, B. H. (1968). Dispersion predictions in natural streams. *Journal of the Sanitary Engineering Division*, 94(SA5), 927–943. <https://doi.org/10.1061/JSEDAI.0000900>
- Garro, B. A., & Vázquez, R. A. (2015). Designing artificial neural networks using particle swarm optimization algorithms. *Computational intelligence and neuroscience*, 2015.
- Ghiasi, B., Jodeiri, A., & Andik, B. (2021). Using a deep convolutional network to predict the longitudinal dispersion coefficient. *Journal of Contaminant Hydrology*, 240, 103798. <https://doi.org/10.1016/j.jconhyd.2021.103798>
- Graf, B. (1995). Observed and predicted velocity and longitudinal dispersion at steady and unsteady flow, Colorado river, Glen canyon dam to lake mead. *Water Resources Bulletin*, 31(2), 265–281. <https://doi.org/10.1111/j.1752-1688.1995.tb03379.x>
- Hornik, K., Stinchcombe, M., & White, H. (1989). Multilayer feedforward networks are universal approximates. *Neural Networks*, 2(5), 359–366. [https://doi.org/10.1016/0893-6080\(89\)90020-8](https://doi.org/10.1016/0893-6080(89)90020-8)
- Iwasa, Y., Aya, S. (1991, May 22–24). Predicting longitudinal dispersion coefficient in open channel flows. In *Proceedings of International Symposium on Environmental Hydraulic* (pp. 505–510), Hong Kong.
- Kargar, K., Samadianfard, S., Parsa, J., Nabipour, N., Shamshirband, S., Mosavi, A., & Kwok-wing Chau, K. (2020). Estimating longitudinal dispersion coefficient in natural streams using empirical models and machine learning algorithms. *Engineering Applications of Computational Fluid Mechanics*, 14(1), 311–322. <https://doi.org/10.1080/19942060.2020.1712260>
- Kashefipour, S. M., & Falconer, R. A. (2002). Longitudinal dispersion coefficients in natural channels. *Water Research*, 36(6), 1596–1608. [https://doi.org/10.1016/S0043-1354\(01\)00351-7](https://doi.org/10.1016/S0043-1354(01)00351-7)
- Li, X., Liu, H., & Yin, M. (2013). Differential evolution for prediction of longitudinal dispersion coefficients in natural streams. *Water resources management*, 27(15), 5245–5260.
- Liu, H. (1977). Predicting dispersion coefficient of streams. *Journal of the Environmental Engineering Division*, 103(1), 59–69. <https://doi.org/10.1061/JEEGAV.0000605>
- Marini, F., & Walczak, B. (2015). Particle swarm optimization (PSO). A tutorial. *Chemometrics and Intelligent Laboratory Systems*, 149, 153–165.
- McQuivey, R. S., & Keefer, T. N. (1974). Simple method for predicting dispersion in streams. *Journal of the Environmental Engineering Division*, 100(4), 997–1011. <https://doi.org/10.1061/JEEGAV.0000247>
- Najafzadeh, M., Noori, R., Afrooz, D., Ghiasi, B., Hosseini-Moghari, S. M., Mirchi, A., Torabi Haghighi, A., & Kløve, B. (2021). A comprehensive uncertainty analysis of model-estimated longitudinal and lateral dispersion coefficients in open channels. *Journal of Hydrology*, 603(A), 126850. <https://doi.org/10.1016/j.jhydrol.2021.126850>
- Najafzadeh, M., & Sattar, A. A. (2015). neuro-fuzzy GMDH approach to predict longitudinal dispersion in water networks. *Water Resources Management*, 29(7), 2205–2219. <https://doi.org/10.1007/s11269-015-0936-8>
- Najafzadeh, M., & Tafarojnoruz, A. (2016). Evaluation of neuro-fuzzy GMDH-based particle swarm optimization to predict longitudinal dispersion coefficient in rivers. *Environmental Earth Sciences*, 75(157), 1–12. <https://doi.org/10.1007/s12665-015-4877-6>
- Noori, R., Deng, Z., Kiaghadi, A., & Kachooosangi, F. T. (2015). How reliable are ANN, ANFIS, and SVM techniques for

- predicting longitudinal dispersion coefficient in natural rivers? *Journal of Hydraulic Engineering*, 04015039.
- Noori, R., Karbassi, A., Farokhnia, A., & Dehghani, M. (2009). Predicting the longitudinal dispersion coefficient using support vector machine and adaptive neuro-fuzzy inference system techniques. *Environmental Engineering Science*, 26(10), 1503–1510. <https://doi.org/10.1089/ees.2008.0360>
- Noori, R., Karbassi, A. R., Mehdizadeh, H., Vesali-Naseh, M., & Sabahi, M. S. (2011). A framework development for predicting the longitudinal dispersion coefficient in natural streams using an artificial neural network. *Environmental Progress & Sustainable Energy*, 30(3), 439–449. <https://doi.org/10.1002/ep.10478>
- Nordin, C. F., & Sabol, G. V. (1974). *Empirical data on longitudinal dispersion in rivers*. US Geological Survey Water Resource Investigation 20–74.
- Parsaie, A., & Haghiabi, A. H. (2015). Predictive modeling of discharge in compound open channel by support vector machine technique. *Modeling Earth Systems and Environment*, 1(34), 1–8. <https://doi.org/10.1007/s40808-015-0002-9>
- Piotrowski, A. P., Rowinski, P. M., & Napiorkowski, J. J. (2012). Comparison of evolutionary computation techniques for noise injected neural network training to estimate longitudinal dispersion coefficients in rivers. *Expert Systems with Applications: An International Journal*, 39(1), 1354–1361. <https://doi.org/10.1016/j.eswa.2011.08.016>
- Qasem, S. N., Samadianfard, S., Kheshtgar, S., Jarhan, S., Kisi, O., Shamshirband, S., & Chau, K. W. (2019). Modeling monthly pan evaporation using wavelet support vector regression and wavelet artificial neural networks in arid and humid climates. *Engineering Applications of Computational Fluid Mechanics*, 13(1), 177–187. <https://doi.org/10.1080/19942060.2018.1564702>
- Riahi-Madvar, H., Ayyoubzadeh, S. A., Khadangi, E., & Ebadzadeh, M. M. (2009). An expert system for predicting longitudinal dispersion coefficient in natural streams by using ANFIS. *Expert Systems with Applications: An International Journal*, 36(4), 8589–8596. <https://doi.org/10.1016/j.eswa.2008.10.043>
- Rutherford, J. C. (1994). *River mixing*. Wiley, p. 347.
- Sahay, R. R. (2011). Prediction of longitudinal dispersion coefficients in natural rivers using artificial neural network. *Environmental Fluid Mechanics*, 11(3), 247–261. <https://doi.org/10.1007/s10652-010-9175-y>
- Samadianfard, S., Hashemi, S., Kargar, K., Izadyar, M., Mostafaeipour, A., Mosavi, A., & Shamshirband, S. (2020). Wind speed prediction using a hybrid model of the multi-layer perceptron and whale optimization algorithm. *Energy Reports*, 6, 1147–1159. <https://doi.org/10.1016/j.egy.2020.05.001>
- Samadianfard, S., Jarhan, S., Salwana, E., Mosavi, A., Shamshirband, S., & Akib, S. (2019b). Support vector regression integrated with fruit Fly optimization algorithm for river flow forecasting in lake Urmia basin. *Water*, 11(9), 1934–1934. <https://doi.org/10.3390/w11091934>
- Samadianfard, S., Majnooni-Heris, A., Qasem, S. N., Kisi, O., Shamshirband, S., & Chau, K. W. (2019a). Daily global solar radiation modeling using data-driven techniques and empirical equations in a semi-arid climate. *Engineering Applications of Computational Fluid Mechanics*, 13(1), 142–157. <https://doi.org/10.1080/19942060.2018.1560364>
- Sattar, A. M. A., & Gharabaghi, B. (2015). Gene expression models for prediction of longitudinal dispersion coefficient in streams. *Journal of Hydrology*, 524, 587–596. <https://doi.org/10.1016/j.jhydrol.2015.03.016>
- Seo, I. W., & Cheong, T. S. (1998). Predicting longitudinal dispersion coefficient in natural streams. *Journal of Hydraulic Engineering*, 124(1), 25–32. [https://doi.org/10.1061/\(ASCE\)0733-9429\(1998\)124:1\(25\)](https://doi.org/10.1061/(ASCE)0733-9429(1998)124:1(25))
- Tayfur, G. (2012). *Soft computing in water resources engineering: Artificial neural networks, fuzzy logic and genetic algorithms*. WIT Press. 288 pages.
- Tayfur, G., & Singh, V. P. (2005). Predicting longitudinal dispersion coefficient in natural streams by artificial neural network. *Journal of Hydraulic Engineering*, 131(11), 991–1000. [https://doi.org/10.1061/\(ASCE\)0733-9429\(2005\)131:11\(991\)](https://doi.org/10.1061/(ASCE)0733-9429(2005)131:11(991))
- Taylor, K. E. (2001). Summarizing multiple aspects of model performance in a single diagram. *Journal of Geophysical Research: Atmospheres*, 106(D7), 7183–7192. <https://doi.org/10.1029/2000JD900719>
- Toprak, Z. F., & Cigizoglu, H. K. (2008). Predicting longitudinal dispersion coefficient in natural streams by artificial intelligence methods. *Hydrological Processes*, 22(20), 4106–4129. <https://doi.org/10.1002/hyp.7012>
- Toprak, Z. F., Hamidi, N., Kisi, O., & Gerger, R. (2014). Modeling dimensionless longitudinal dispersion coefficient in natural streams using artificial intelligence methods. *KSCE Journal of Civil Engineering*, 18(2), 718–730. <https://doi.org/10.1007/s12205-014-0089-y>
- Toprak, Z. F., Sen, Z., & Savci, M. E. (2004). Comment on “longitudinal dispersion coefficients in natural channels”. *Water Research*, 38(13), 3139–3143. <https://doi.org/10.1016/j.watres.2003.08.004>
- Tsuruoka, Y., Tsujii, J., & Ananiadou, S. (2009, September 12–16). Stochastic gradient descent training for L1-regularized log-linear models with cumulative penalty. In *47th annual meeting of the ACL and the 4th IJCNLP of the AFNLP* (pp. 477e485).
- Tutmez, B., & Yuceer, M. (2013). Regression kriging analysis for longitudinal dispersion coefficient. *Water Resources Management*, 27(9), 3307–3318. <https://doi.org/10.1007/s11269-013-0348-6>
- Ulke, A., Tayfur, G., & Ozkul, S. (2009). Predicting suspended sediment loads and missing data for gediz river, Turkey. *Journal of Hydrologic Engineering*, 14(9), 954–965. [https://doi.org/10.1061/\(ASCE\)HE.1943-5584.0000060](https://doi.org/10.1061/(ASCE)HE.1943-5584.0000060)
- Wang, Y., Huai, W., & Wang, W. (2017). Physically sound formula for longitudinal dispersion coefficients of natural rivers. *Journal of Hydrology*, 544, 511–523. <https://doi.org/10.1016/j.jhydrol.2016.11.058>
- Zeng, Y., & Huai, W. (2014). Estimation of longitudinal dispersion coefficient in rivers. *Journal of Hydro-Environment Research*, 8(1), 2–8.
- Zeng, Y., Huai, W., & Zhao, M. (2016). Flow characteristics of rectangular open channels with compound vegetation roughness. *Applied Mathematics and Mechanics*, 37(3), 341–348.
- Zounemat-Kermani, M., Seo, Y., Kim, S., Ghorbani, M. A., Samadianfard, S., Naghsara, S., Kim, N. W., & Singh, V. P. (2019). Can decomposition approaches always enhance soft computing models? Predicting the dissolved oxygen concentration in the St. Johns River, Florida. *Applied Sciences*, 9(12), 2534–2534. <https://doi.org/10.3390/app9122534>

Appendix

NO	Stream	W (m)	H (m)	$U(m/s)$	$U_*(m/s)$	$\varepsilon(m^2/s)$
1	Copper Creep, VA (below guage)	15.9	0.49	0.21	0.079	19.52
2	Copper Creep, VA (below guage)	18.3	0.84	0.52	0.1	21.4
3	Copper Creep, VA (below guage)	16.2	0.49	0.25	0.079	9.5
4	Clinch River, TN (below gage)	46.9	0.86	0.28	0.067	13.93
5	Clinch River, TN (below gage)	59.4	2.13	0.86	0.104	53.88
6	Clinch River, TN (below gage)	53.3	20.9	0.79	0.107	46.45
7	Copper Creek, VA (above gage)	18.6	0.39	0.14	0.116	9.85
8	Power River, TN	33.8	0.85	0.16	0.055	9.5
9	Clinch River, VA	36	0.58	0.3	0.049	8.08
10	Green and Duwamish	21.77	1.58	0.31	0.058	6.5
11	Green and Duwamish	29.61	1.08	0.36	0.048	0.5
12	Bayou Anacoco	19.8	0.41	0.29	0.044	13.94
13	Nooksack River	86	2.94	1.2	0.514	153.29
14	Antietam Creek	15.8	0.39	0.32	0.06	9.29
15	Antietam Creek	19.8	0.52	0.43	0.069	16.26
16	Antietam Creek	24.4	0.71	0.52	0.081	25.55
17	Monocacy River	35.1	0.32	0.21	0.04	4.65
18	Monocacy River	36.6	0.45	0.32	0.05	13.94
19	Monocacy River	47.5	0.87	0.44	0.07	37.16
20	Missouri River	182.9	2.23	0.93	0.065	464.52
21	Missouri River	201.2	3.56	1.27	0.082	836.13
22	Missouri River	196.6	3.11	1.53	0.077	891.87
23	Wind/Bighorn Rivers	67.1	0.98	0.88	0.11	41.81
24	Elkhorn River	32.6	0.3	0.43	0.046	9.29
25	Elkhorn River	50.9	0.42	0.46	0.046	20.9
26	John day River	25	0.56	1.01	0.137	13.94
27	Comite River	12.5	0.26	0.31	0.043	6.97
28	Comite River	15.8	0.41	0.37	0.055	13.94
29	Amite River	36.6	0.81	0.29	0.068	23.23
30	Amite River	42.4	0.8	0.42	0.068	30.19
31	Sabine River	103.6	2.04	0.56	0.054	315.87
32	Sabine River	127.4	4.75	0.64	0.081	668.9
33	Muddy Creek	13.4	0.81	0.37	0.077	13.94
34	Muddy Creek	19.5	1.2	0.45	0.093	32.52
35	Sabine River, Texas	35.1	0.98	0.21	0.041	39.48
36	White River	67.1	0.55	0.35	0.044	30.19
37	Chattahoochee River	65.5	1.13	0.39	0.075	32.52
38	Susquehanna River	202.7	1.35	0.39	0.065	92.9
39	Antietam Creek	10.97	0.52	0.21	0.075	17.5
40	Antietam Creek	23.47	0.7	0.52	0.101	101.5
41	Antietam Creek	24.99	0.45	0.41	0.081	25.9
42	Antietam Creek	12.8	0.3	0.42	0.057	17.5
43	Antietam Creek	24.08	0.98	0.59	0.098	101.5
44	Antietam Creek	11.89	0.66	0.43	0.085	20.9
45	Antietam Creek	21.03	0.48	0.52	0.069	25.9
46	Monocacy River	48.7	0.55	0.26	0.05	37.8
47	Monocacy River	92.96	0.71	0.16	0.05	41.4
48	Monocacy River	51.21	0.65	0.62	0.04	29.6
49	Monocacy River	97.54	1.15	0.32	0.058	119.8
50	Monocacy River	49.99	0.95	0.32	0.075	29.6
51	Monocacy River	33.53	0.58	0.16	0.041	66.5
52	Monocacy River	40.54	0.41	0.23	0.04	66.5
53	Conococheague Creek	42.21	0.69	0.23	0.064	40.8
54	Conococheague Creek	49.68	0.41	0.15	0.081	29.3
55	Conococheague Creek	42.98	1.13	0.63	0.081	53.3
56	Conococheague Creek	43.28	0.69	0.22	0.064	40.8
57	Conococheague Creek	63.7	0.46	0.1	0.056	29.3
58	Conococheague Creek	59.44	0.76	0.68	0.072	53.3
59	Chattahoochee River	75.6	1.95	0.74	0.138	88.9
60	Chattahoochee River	91.9	2.44	0.52	0.094	166.9
61	Chattahoochee River	99.97	2.5	0.3	0.105	166.9
62	Salt Creek	32	0.5	0.24	0.038	52.2
63	Difficult Run	14.5	0.31	0.25	0.062	1.9
64	Difficult Run	11.58	0.4	0.22	0.087	1.9

(continued)

Appendix. Continued.

NO	Stream	W (m)	H (m)	$U(m/s)$	$U_*(m/s)$	$\varepsilon(m^2/s)$
65	Bear Creek	13.7	0.85	1.29	0.553	2.9
66	Little Pincy Creek	15.9	0.2	0.39	0.053	7.1
67	Bayou Anacoco	17.5	0.45	0.32	0.024	5.8
68	Bayou Anacoco	25.9	0.94	0.34	0.067	27.6
69	Bayou Anacoco	36.6	0.91	0.4	0.067	40.2
70	Comite River	15.7	0.2	0.36	0.04	69
71	Comite River	6.1	0.49	0.25	0.058	69
72	Bayou Bartholomew	33.4	1.4	0.2	0.03	54.7
73	Bayou Bartholomew	37.49	2.07	0.1	0.04	54.7
74	Amite River	21.3	0.5	0.54	0.027	501.4
75	Amite River	46.02	0.53	0.41	0.043	501.4
76	Tickfau River	14.9	0.59	0.27	0.08	10.3
77	Tickfau River	41.45	1.04	0.07	0.09	10.3
78	Tangipahoa River	31.4	0.81	0.48	0.072	45.1
79	Tangipahoa River	29.9	0.4	0.34	0.02	44
80	Tangipahoa River	42.98	1.28	0.26	0.068	45.1
81	Tangipahoa River	31.7	0.76	0.36	0.053	44
82	Red River	253.6	0.81	0.48	0.072	45.1
83	Red River	161.5	0.4	0.34	0.02	44
84	Red River	152.4	1.62	0.61	0.032	143.8
85	Red River	155.1	3.96	0.29	0.06	130.5
86	Red River	248.11	4.82	0.31	0.065	143.8
87	Sabine River, LA	116.4	3.66	0.45	0.057	227.6
88	Sabine River, LA	160.3	1.74	0.47	0.036	177.7
89	Sabine River, TX	14.2	1.65	0.58	0.054	131.3
90	Sabine River, TX	12.2	2.32	1.06	0.054	308.9
91	Sabine River, TX	21.3	0.5	0.13	0.037	12.8
92	Sabine River, TX	21.64	0.61	0.08	0.042	12.8
93	Sabine River, TX	17.37	1.23	0.04	0.05	14.7
94	Sabine River, TX	31.39	1.43	0.13	0.041	24.2
95	Wind/Bighom Rivers	44.2	1.4	0.99	0.14	184.6
96	Wind/Bighom Rivers	85.3	2.4	1.73	0.15	464.6
97	Copper Creek	16.7	0.5	0.2	0.08	16.8
98	Clinch River	48.5	1.2	0.21	0.07	14.8
99	Copper Creek	18.3	0.4	0.15	0.12	20.7
100	Powell River	36.8	0.9	0.13	0.05	15.5
101	Clinch River	28.7	0.6	0.35	0.07	10.7
102	Copper Creek	19.6	0.8	0.49	0.1	20.8
103	Clinch River	57.9	2.5	0.75	0.1	40.5
104	Conchela Canal	24.7	1.6	0.66	0.04	5.9
105	Clinch River	33.53	0.78	0.19	0.049	10.7
106	Clinch River	55.78	2.26	0.69	0.099	36.93
107	Clinch River	53.2	2.4	0.66	0.11	36.9
108	Coachell Canal, CA	23.77	1.6	0.67	0.04	5.96
109	Coachell Canal, CA	24.99	1.54	0.66	0.037	5.92
110	Copper Creek	16.8	0.5	0.24	0.08	24.6
111	Missouri River	180.6	3.3	1.62	0.08	1486.5
112	Bayou Anacoco	25.9	0.9	0.34	0.07	32.5
113	Bayou Anacoco	36.6	0.9	0.4	0.07	39.5
114	Nooksack River	64	0.8	0.67	0.27	34.8
115	Wind/Bighom Rivers	59.4	1.1	0.88	0.12	41.8
116	Wind/Bighom Rivers	68.6	2.2	1.55	0.17	162.6
117	John Day River	34.1	2.5	0.82	0.18	65
118	Yadkin River	70.1	2.4	0.43	0.1	111.5
119	Yadkin River	71.6	3.8	0.76	0.13	260.1
120	Colorado River	106.1	6.1	0.79	0.088	181
121	Colorado River	71.6	8.2	1.2	0.337	243
122	Albert	100	4.4	0.029	0.0016	0.2
123	Dessel-Herentals	35	2.5	0.037	0.0022	0.2
124	Yuma Mesa A	7.6	3.45	0.68	0.047	0.5
125	Bocholt-Dessel	35	2.5	0.107	0.0063	1.4
126	Villemsvaart	34	2.5	0.13	0.0079	1.7

(continued)

Appendix. Continued.

NO	Stream	W (m)	H (m)	$U(m/s)$	$U_*(m/s)$	$\varepsilon(m^2/s)$
127	Chicago Ship Canal	49	8.07	0.27	0.019	3
128	Irrigation	1.4	0.19	0.38	0.11	9.6
129	Irrigation	1.5	0.14	0.33	0.1	1.9
130	Puneha	5	0.28	0.26	0.21	7.2
131	Kapuni	9	0.3	0.37	0.15	8.4
132	Kapuni	10	0.35	0.53	0.17	12.4
133	Manganui	20	0.4	0.19	0.18	6.5
134	Waiongana	13	0.6	0.48	0.24	6.8
135	Stony	10	0.63	0.55	0.3	13.5
136	Waiotapu	11.4	0.75	0.41	0.061	8
137	Manawatu	59	0.72	0.37	0.07	32
138	Manawatu	63	1	0.32	0.094	22
139	Manawatu	60	0.95	0.46	0.092	47
140	Tarawera	25	1.21	0.73	0.084	27
141	Tarawera	20	1.92	0.62	0.123	11.5
142	Tarawera	25	1.38	0.77	0.091	20.5
143	Tarawera	25	1.4	0.78	0.091	15.5
144	Tarawera	25	1.57	0.83	0.096	18
145	Tarawera	85	2.6	0.69	0.06	52
146	Waikato	120	2	0.64	0.05	67
147	Miljacka	11	0.29	0.35	0.058	2.7
148	Upper Tame	9.9	0.83	0.46	0.09	5.5
149	Upper Tame	9.9	0.92	0.52	0.1	5.1